Orbital Symmetry and Electron Correlation in Na_xCoO_2

W. B. Wu,[1,2] D. J. Huang,[1,2,*] J. Okamoto,[1] A. Tanaka,[3] H.-J. Lin,[1] F. C. Chou,[4] A. Fujimori,[5] and C. T. Chen[1]

[1]*National Synchrotron Radiation Research Center, Hsinchu 30076, Taiwan*
[2]*Department of Electrophysics, National Chiao-Tung University, Hsinchu 30010, Taiwan*
[3]*Department of Quantum Matters, ADSM, Hiroshima University, Higashi-Hiroshima 739-8530, Japan*
[4]*Center for Materials Science and Engineering, Massachusetts Institute of Technology, Cambridge, Massachusetts 02139, USA*
[5]*Department of Complexity Science and Engineering, University of Tokyo, Chiba 277-8561, Japan*

(Received 14 August 2004; published 14 April 2005)

Measurements of polarization-dependent soft x-ray absorption reveal that the electronic states determining the low-energy excitations of Na_xCoO_2 have predominantly a_{1g} symmetry with significant O $2p$ character. In contrast to the prediction of band theory, doping-dependent O $1s$ x-ray absorption shows a large transfer of spectral weight, providing spectral evidence for strong electron correlations of the layered cobaltates. We also found that Na_xCoO_2 exhibits a charge-transfer electronic character rather than a Mott-Hubbard character.

DOI: 10.1103/PhysRevLett.94.146402 PACS numbers: 71.27.+a, 71.70.–d, 74.70.–b, 78.70.Dm

Sodium cobalt oxides (Na_xCoO_2) have attracted renewed interest because of their exceptionally large thermoelectric power [1] and the discovery of superconductivity in their hydrated counterparts [2]. Despite intensive experimental [1–9] and theoretical [10–21] works, there remain many unresolved issues concerning the electronic structure of Na_xCoO_2.

An important issue is the orbital character of the valence electrons responsible for low-energy excitations. The lattice of Na_xCoO_2 exhibits a trigonal distortion, leading to a splitting of t_{2g} states into e_g' and a_{1g} states, as shown in Fig. 1. The e_g' states spread over the ab plane, whereas the a_{1g} state extends to the c axis [22]. Band-structure calculations in the local-density approximation (LDA) show that the a_{1g} state has a one-particle energy higher than that of e_g' and is most relevant to low-energy excitations [10]. These calculations are however different from a crystal-field approach in which the compressed trigonal distortion stabilizes the a_{1g} state [16], as illustrated in Fig. 1(b).

Several theoretical works have proposed one-band models to discuss the electronic structure of Na_xCoO_2 [12–15], rather than multiband models [16,17]. The validity of one-band models is a fundamental question for the triangular cobaltates. If the twofold e_g' level is higher than the a_{1g} level, the orbital degree of freedom is an indispensable ingredient in understanding the electronic states of the material. On the other hand, the states near the Fermi level can be mapped onto a single-band model on the triangular lattice when the a_{1g} level is higher.

To comprehend the effect of electron correlations is also imperative to have an understanding of the electronic structure of Na_xCoO_2. Many microscopic models with strong electron correlations explicitly included have been proposed to explain the spectacular properties of Na_xCoO_2 [12–17]. On the other hand, a recent LDA + U study (LDA including on-site Coulomb energy U) [21] explains the Fermi surface measured by angle-resolved photoemission [8,9] and concludes that Na_xCoO_2 is a moderately correlated system. One therefore requires further spectral evidence for strong electron correlations to justify microscopic models of correlated electrons for Na_xCoO_2.

Another subject is whether the electronic states of Na_xCoO_2 responsible for low-energy excitations have O $2p$ character. Early LDA calculations [10] indicate that hybridization between Co $3d$ and O $2p$ in $Na_{0.5}CoO_2$ is weak. Analysis of core-level photoemission results suggests that Na_xCoO_2 has a Mott-Hubbard-like rather than a charge-transfer electronic structure [6]. On the other hand, LDA results corroborated with a Hubbard-like model conclude that $Na_{1/3}CoO_2$ exhibits significant hybridization between Co $3d$ and O $2p$ [18].

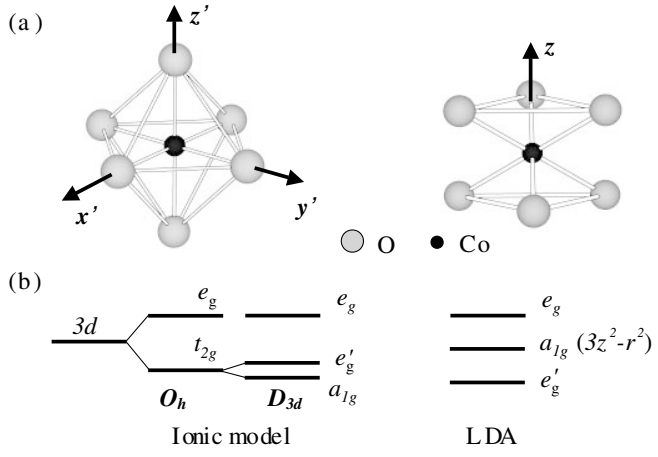

FIG. 1. (a) Illustration of the trigonal distortion of a CoO_6 octahedron. Left panel: undistorted CoO_6 octahedron with cubic (O_h) symmetry. Right panel: compressed CoO_6 octahedron with D_{3d} symmetry. The distorted CoO_6 is rotated such that the threefold rotation axis is along the c axis. (b) Crystal-field splitting of Co $3d$ states in distorted CoO_6 according to an ionic model and relative energy positions of $3d$ bands obtained from LDA calculations.

In this Letter, we present measurements of soft x-ray absorption spectroscopy (XAS) on Na_xCoO_2 pertinent to its orbital character of the electronic states determining the low-energy physics. To investigate the detailed electronic structure, we discuss the spectral character of strongly correlated electrons of Na_xCoO_2. We also compare Co $2p$ XAS with calculations using a cluster model in the configuration-interaction (CI) approach.

We measured XAS on Na_xCoO_2 using the Dragon beamline at the National Synchrotron Radiation Research Center in Taiwan. Single crystals of $Na_{0.75}CoO_2$ were grown by the traveling solvent floating-zone method. Crystals with smaller Na concentrations of $x = 0.67$ and 0.5 were prepared from $Na_{0.75}CoO_2$ through subsequent electrochemical deintercalation procedures. Details of crystal growth are discussed elsewhere [23]. Crystals were freshly cleaved in vacuum with a pressure lower than 5×10^{-10} torr at 80 K. XAS were recorded through collecting the sample drain current. The incident angle was 60° from the sample surface normal; the photon energy resolutions were set at 0.12 eV and 0.25 eV for photon energies of 530 eV and 780 eV, respectively. In polarization-dependent measurements, we rotated the sample about the direction of incident photons to eliminate experimental artifacts related to the difference in the optical path and to the probing area. All measured XAS referred to the **E** vector of photons parallel to the crystal c axis ($I_\parallel$) are shown with a correction for the geometric effect, $I_\parallel = \frac{4}{3}(I - \frac{1}{4}I_\perp)$, in which $I_\perp$ and I are measured XAS with $\mathbf{E} \perp c$ and with **E** in the plane defined by the c axis and the direction of incident radiation, respectively.

Figure 2 presents isotropic O $1s$ XAS of $Na_{0.5}CoO_2$ single crystals; our spectrum is similar to those of polycrystalline samples [24]. O $1s$ XAS measures transitions from an O $1s$ core level to unoccupied O $2p$ states mixing with bands of primary Co or Na character. The structure in XAS near the threshold arises from covalent mixing of Co $3d$ and O $2p$. One can interpret such a near-edge structure as a one-electron addition process, i.e., $d^n \rightarrow d^{n+1}$, if the influence of the O $1s$ core hole is neglected [25,26]. We observed three pronounced O $1s$ XAS peaks in the vicinity of the threshold, implying strong hybridization between O $2p$ and Co $3d$ and many O $2p$ holes existing in $Na_{0.5}CoO_2$. The broad feature about 540 eV corresponds to Co $4sp$ bands; the features in the region about 535 eV are attributed to transitions involving Na $3p$.

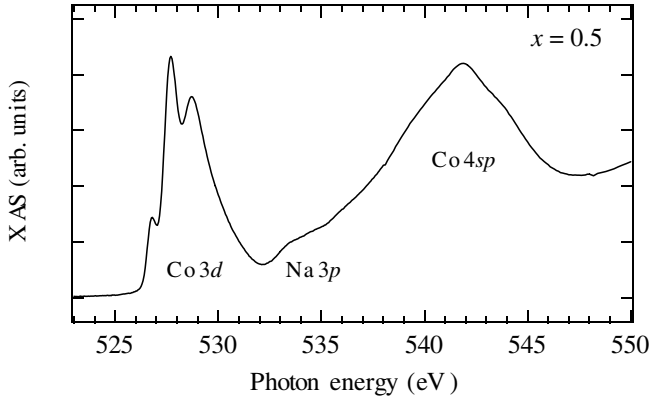

FIG. 2. O $1s$ XAS spectrum of $Na_{0.5}CoO_2$ measured in the total electron yield mode. The unoccupied bands with which O $2p$ states hybridize are denoted in the plot.

As for determining the symmetry of electronic states governing the low-energy excitations, we resorted to measurements of polarization-dependent O $1s$ XAS of $Na_{0.5}CoO_2$, as plotted in Fig. 3. The O $1s$ XAS shows that the lowest-energy peak at 526.8 eV (labeled as A) has a strong z component. The ratio $I_\perp/I_\parallel$ for peak A is 0.37 ± 0.05, as depicted in the inset of Fig. 3. The in-plane components of two other peaks at 527.6 eV and 528.7 eV (labeled as A' and B, respectively) are slightly larger than their corresponding z components.

The polarization dependencies of peaks A, A', and B in the O $1s$ XAS depend on hybridization between Co $3d$ and O $2p$. Qualitatively, the hybridization results from the interatomic matrix element V_{pd} between Co $3d$ and O $2p$, which can be expressed in terms of the Slater-Koster transfer integrals $pd\sigma$ and $pd\pi$ [27]; the ratio $I_\perp/I_\parallel$ is propor-

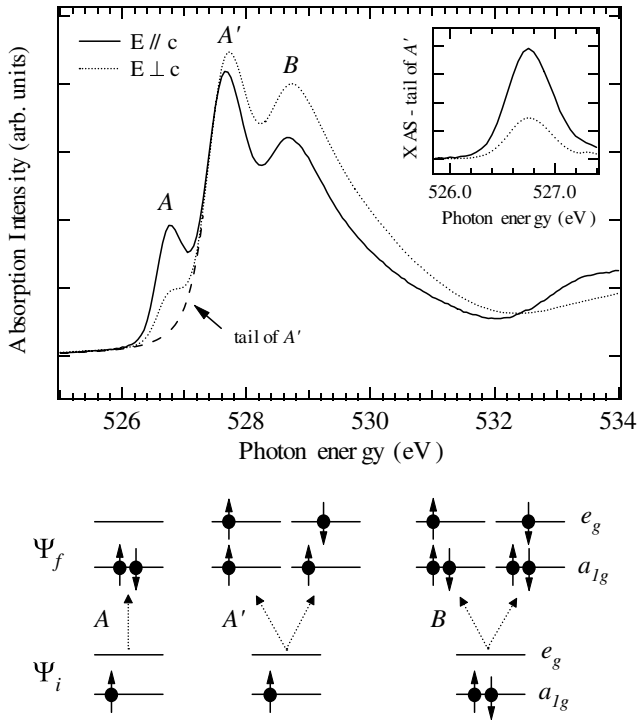

FIG. 3. Upper panel: Polarization-dependent O $1s$ XAS of $Na_{0.5}CoO_2$ with $\mathbf{E} \perp c$ (dotted line) and $\mathbf{E} \parallel c$ (solid line). The inset shows the XAS of peak A after removal of background from the tail of peak A' (dashed line). Lower panel: Energy diagrams illustrating transitions from Ψ_i in the low-spin state to Ψ_f corresponding to the symmetries of peaks A, A', and B. The e_g' states are omitted for clarity.

tional to the ratio of the averaged V_{pd}^2 with O $2p$ orbitals perpendicular and parallel to the c axis. For an undistorted lattice, $I_\perp/I_\parallel$ of O $1s$ XAS with a final state of a_{1g} symmetry is 0.25, while that of e_g symmetry is 1.0, if one uses an empirical relation $pd\sigma = -(4/\sqrt{3})pd\pi$. $I_\perp/I_\parallel$ depends also on the distortion and the band effect. If the compressed trigonal distortion of a Na_xCoO_2 lattice is taken into account, O $1s$ XAS with final states of a_{1g} symmetry has a large out-of-plane polarization, whereas that with e_g symmetry has an in-plane polarization. Thus, our measurements that peak A and A' have opposite polarizations show that peak A results predominantly from adding an electron to a state of a_{1g} symmetry, whereas peaks A' and B correspond to adding electrons to states of e_g symmetry, as illustrated in the lower panel of Fig. 3. In other words, the symmetries of the transitions associated with peaks A, A', and B correspond mainly to $(a_{1g})^1 \rightarrow (a_{1g})^2$, $(a_{1g})^1 \rightarrow (a_{1g})^1(e_g)^1$, and $(a_{1g})^2 \rightarrow (a_{1g})^2(e_g)^1$, respectively. Note that we omit the low-spin $(e_g')^4$ in the above expressions for clarity. These observations reveal that the electronic states of predominantly a_{1g} symmetry determine the low-energy excitations of Na_xCoO_2. Moreover, our observation of the a_{1g} symmetry of the states crossing the Fermi level suggests a significant hybridization between O $2p$ and Co $3d$, because hopping of a_{1g} states within the CoO_2 layer would be difficult without O $2p$ mixing. Hence, one expects that the ground-state configurations for Co^{4+} and Co^{3+} in Na_xCoO_2 have significant weights of $d^6\underline{L}$ and $d^7\underline{L}$, respectively, in which $\underline{L}$ denotes an oxygen $2p$ hole.

To seek spectral evidence for electron correlations of $3d$ bands, we plot doping-dependent isotropic O $1s$ XAS of Na_xCoO_2 in Fig. 4. The spectra are normalized to have the same intensity at 600 eV at which O $1s$ XAS has no doping-dependent structure. We found a spectral-weight transfer in the doping-dependent O $1s$ XAS; as the doping x increases, the intensities of peaks A and A' decrease, but peak B increases in intensity. Such a spectral-weight transfer is in contrast to the picture of rigid-band shift in which the spectral weight associated with a_{1g} bands is influenced only by the position of the Fermi level. The decrease (increase) in the intensity of peaks A and A' (peak B) with the increase of doping indicates that the XAS peaks are derived from Co^{4+} (Co^{3+}), because a fraction x of Co^{4+} changes to Co^{3+} when the hypothetical CoO_2 is doped with Na. Our results thus suggest that the peaks A and A' (peak B) originate from O $2p$ hybridized with $3d$ states of Co^{4+} (Co^{3+}) and correspond to adding electrons to the states of a_{1g} and e_g symmetries associated with Co^{4+} (e_g symmetry associated with Co^{3+}), further supporting the symmetry assignment from the polarization-dependent measurements discussed above. The spectral-weight transfer of the one-electron addition observed in Na_xCoO_2 is a general feature of strongly correlated systems [28], as in

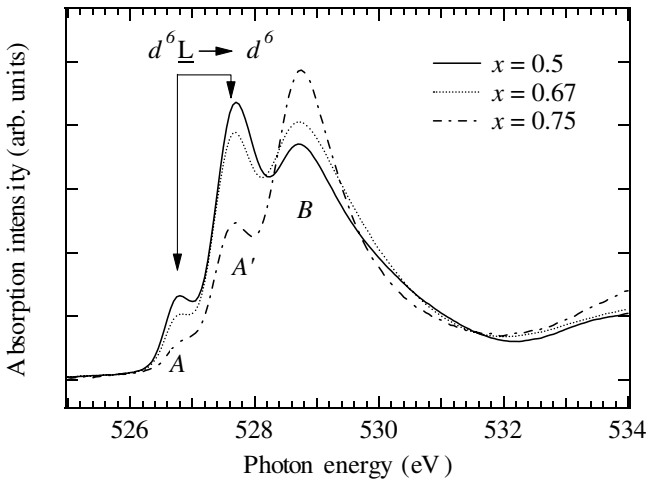

FIG. 4. Doping-dependent isotropic O $1s$ XAS of Na_xCoO_2, i.e., $(I_\parallel + I_\perp)/2$. The dominant transitions $d^6\underline{L} \rightarrow d^6$ leading to the peaks A and A' are indicated in the figure.

electron-energy loss experiments [29] and O $1s$ XAS [30] study of $La_{2-x}Sr_xCuO_4$. Such behavior has been found in Li-doped NiO as well [31]. Both $La_{2-x}Sr_xCuO_4$ and $Li_xNi_{1-x}O$ are charge-transfer systems; thus Na_xCoO_2 is expected to have a charge-transfer electronic structure.

Spectral-weight transfer observed in O $1s$ XAS also manifests the doping-dependent p-d hybridization in Na_xCoO_2. The p-d hybridization determines the e_g occupation in the ground state and the change in the O $1s$ XAS intensities of different Na concentrations. As the Na doping changes from $x = 0.5$ to $x = 0.75$, the increase in the intensity of peak B is smaller than the decrease of peak A', demonstrating the reduction of p-d hybridization and e_g occupation with the increase of doping. Our results agree with recent LDA calculations [18] which conclude that, as the doping increases, the increase of t_{2g} electrons are dressed by e_g holes.

We measured also the Co $L_{2,3}$ edge XAS of Na_xCoO_2 to further study its detailed electronic structure. Based on a cluster model in the CI approach, we simulated XAS spectra with a superposition of calculated XAS for Co^{4+} and Co^{3+} with weights of $1 - x : x$. Details of the calculations will be presented elsewhere. To summarize, the shoulder peak on the low-energy side of the L_3 edge arises from the a_{1g} orbital character in the ground state. Comparing the Co L-edge XAS of $x = 0.5$, 0.67, and 0.75 with CI calculations using a series of parameters, we found that the calculated XAS for Co ions in a low-spin (LS) state resembles the measured XAS satisfactorily, but the calculated XAS for high-spin (HS) ions is inconsistent with the measurement, as demonstrated in Fig. 5 for $x = 0.5$ [32]. The calculations indicate that Na_xCoO_2 has a charge-transfer energy smaller than the on-site Coulomb energy ($U_{dd} = 4.5$ eV). In particular, because of the high valency, Co^{4+} ions have a negative charge-transfer energy

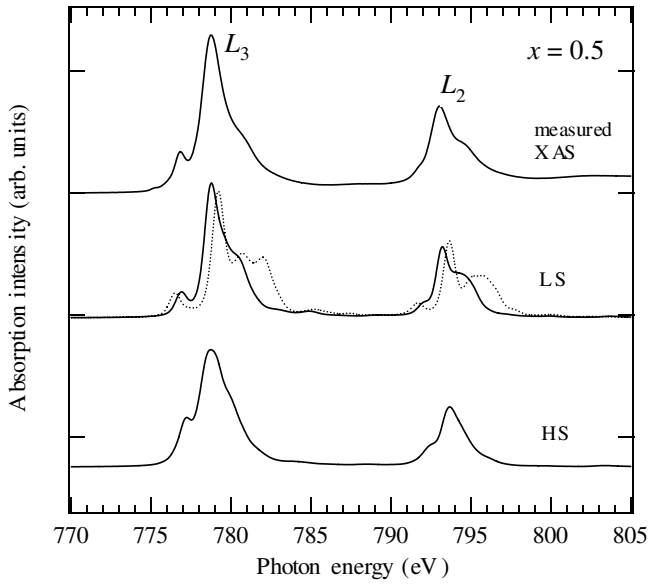

FIG. 5. Measured and calculated isotropic Co L-edge XAS of $Na_{0.5}CoO_2$. Theoretical Co L-edge XAS spectra for LS and HS Co $3d$ states were broadened with a Gaussian full width of 0.5 eV at half maximum (FWHM) and with a Lorentian FWHM of 0.4 eV. The dotted line is a simulated XAS with the parameters reported in Ref. [6].

($\Delta \sim -1$ eV) [33], in contrast to the conclusion from the analysis of core-level photoemission data [6]. Calculations with the parameters that Chainani *et al.* concluded ($U_{dd} = 5.5$, $\Delta = 4.0$, $10Dq = 2.5$ for Co^{3+}, and $10Dq = 4.0$ for Co^{4+} in units of eV [6]) give rise to a Co $2p$ XAS inconsistent with our measurements, as in Fig. 5. Thus Na_xCoO_2 exhibits a charge-transfer electronic character rather than a Mott-Hubbard character; the $d^6\underline{L}$ configuration dominates the ground state of Co^{4+} in Na_xCoO_2 [34], like Co^{4+} in $SrCoO_3$ [35] and $La_{1-x}Sr_xCoO_3$ [36]. These results suggest that peaks A and A' of Fig. 4 are derived from transitions of $d^6\underline{L} \rightarrow d^6$ and that the empty a_{1g} band to which the doped electrons go has predominantly O $2p$ character for $x \geq 0.5$.

In conclusion, measurements of doping-dependent O $1s$ XAS provide a spectral fingerprint for strong electron correlations of Na_xCoO_2. Our results reveal the charge-transfer electronic character of Na_xCoO_2; the doping of Na strongly affects the O $2p$ hole density. The electronic states responsible for the low-energy excitations of Na_xCoO_2 have predominantly a_{1g} symmetry with significant O $2p$ character.

We thank F. C. Zhang, C. Y. Mou, G. Kotliar, G. Y. Guo, and L. H. Tjeng for valuable discussions. This work was supported in part by the National Science Council of Taiwan and by the MRSEC Program of the National Science Foundation of the U.S. under Grant No. DMR-02-13282.

*Corresponding author.
Electronic address: djhuang@nsrrc.org.tw

[1] I. Terasaki, Y. Sasago, and K. Uchinokura, Phys. Rev. B **56**, R12685 (1997).
[2] K. Takada *et al.*, Nature (London) **422**, 53 (2003).
[3] R. Ray *et al.*, Phys. Rev. B **59**, 9454 (1999).
[4] Y. Wang *et al.*, Nature (London) **423**, 425 (2003).
[5] T. Motohashi *et al.*, Phys. Rev. B **67**, 064406 (2003).
[6] A. Chainani *et al.*, Phys. Rev. B **69**, 180508(R) (2004).
[7] M. L. Foo *et al.*, Phys. Rev. Lett. **92**, 247001 (2004).
[8] M. Z. Hasan *et al.*, Phys. Rev. Lett. **92**, 246402 (2004).
[9] H.-B. Yang *et al.*, Phys. Rev. Lett. **92**, 246403 (2004).
[10] D. J. Singh, Phys. Rev. B **61**, 13 397 (2000).
[11] D. J. Singh, Phys. Rev. B **68**, 020503(R) (2003).
[12] Y. Tanaka, Y. Yanase, and M. Ogata, cond-mat/0311266.
[13] G. Baskaran, Phys. Rev. Lett. **91**, 097003 (2003).
[14] Q.-H. Wang, D.-H. Lee, and P. A. Lee, Phys. Rev. B **69**, 092504 (2004).
[15] B. Kumar and B. S. Shastry, Phys. Rev. B **68**, 104508 (2003); O. I. Motrunich and Patrick A. Lee, *ibid.* **69**, 214516 (2004).
[16] W. Koshibae and S. Maekawa, Phys. Rev. Lett. **91**, 257003 (2003).
[17] Y. Yanase, M. Mochizuki, and M. Ogata, cond-mat/0407563.
[18] C. A. Marianetti, G. Kotliar, and G. Ceder, Phys. Rev. Lett. **92**, 196405 (2004).
[19] L. J. Zou, J.-L. Wang, and Z. Zeng, Phys. Rev. B **69**, 132505 (2004).
[20] P. Zhang *et al.*, Phys. Rev. B **70**, 085108 (2004).
[21] P. Zhang *et al.*, Phys. Rev. Lett. **93**, 236402 (2004).
[22] If the z axis is along the c axis, a_{1g} is $d_{3z^2-r^2}$; e'_g are $\frac{1}{\sqrt{3}} \times (d_{yz} + \sqrt{2}d_{xy})$ and $\frac{1}{\sqrt{3}}(d_{zx} - \sqrt{2}d_{x^2-y^2})$.
[23] F. C. Chou *et al.*, Phys. Rev. Lett. **92**, 157004 (2004).
[24] W.-S. Yoon *et al.*, J. Phys. Chem. B **106**, 2526 (2002); M. Kubota *et al.*, Phys. Rev. B **70**, 012508 (2004).
[25] F. M. F. de Groot *et al.*, Phys. Rev. B **40**, 5715 (1989).
[26] J. van Elp and A. Tanaka, Phys. Rev. B **60**, 5331 (1999).
[27] J. C. Slater and G. F. Koster, Phys. Rev. **94**, 1498 (1954).
[28] H. Eskes, M. B. J. Meinders, and G. A. Sawatzky, Phys. Rev. Lett. **67**, 1035 (1991).
[29] H. Romberg *et al.*, Phys. Rev. B **42**, 8768 (1990).
[30] C. T. Chen *et al.*, Phys. Rev. Lett. **66**, 104 (1991).
[31] P. Kuiper *et al.*, Phys. Rev. Lett. **62**, 221 (1989).
[32] Parameters (in units of eV): $U_{dd} = 4.5$, $U_{dc} = 5.5$, $\Delta = 3.5$ (for Co^{3+}), $\Delta = -1.0$ (for Co^{4+}), $10Dq = 1.5$ (for LS), $10Dq = 0.5$ (for HS), $V_{eg} = 3.5$, $T_{pp} = 0.7$, $D_{trg} = -1.0$, and $Q_{mix} = 0.5$, where $D_{trg} \equiv E(e'_g) - E(a_{1g})$; Q_{mix} is the hybridization between e'_g and e_g.
[33] Δ for Co^{4+} is defined as $E(3d^6\underline{L}) - E(3d^5)$.
[34] The ground-state configurations for LS Co^{4+} are $d^5 = 15.9\%$, $d^6\underline{L} = 48.1\%$, $d^7\underline{L}^2 = 31.1\%$, and $d^8\underline{L}^3 = 4.9\%$; those for LS Co^{3+} are $d^6 = 43.2\%$, $d^7\underline{L} = 46.9\%$, and $d^8\underline{L}^2 = 9.9\%$.
[35] R. H. Potze, G. A. Sawatzky, and M. Abbate, Phys. Rev. B **51**, 11 501 (1995).
[36] T. Saitoh *et al.*, Phys. Rev. B **56**, 1290 (1997).